

Nanochannel-Based Poration Drives Benign and Effective Nonviral Gene Delivery to Peripheral Nerve Tissue

Jordan T. Moore, Christopher G. Wier, Luke R. Lemmerman, Lilibeth Ortega-Pineda, Daniel J. Dodd, William R. Lawrence, Silvia Duarte-Sanmiguel, Kavya Dathathreya, Ludmila Diaz-Starokozheva, Hallie N. Harris, Chandan K. Sen, Ian L. Valerio, Natalia Higueta-Castro, William David Arnold, Stephen J. Kolb, and Daniel Gallego-Perez*

While gene and cell therapies have emerged as promising treatment strategies for various neurological conditions, heavy reliance on viral vectors can hamper widespread clinical implementation. Here, the use of tissue nanotransfection as a platform nanotechnology to drive nonviral gene delivery to nerve tissue via nanochannels, in an effective, controlled, and benign manner is explored. TNT facilitates plasmid DNA delivery to the sciatic nerve of mice in a voltage-dependent manner. Compared to standard bulk electroporation (BEP), impairment in toe-spread and pinprick response is not caused by TNT, and has limited to no impact on electrophysiological parameters. BEP, however, induces significant nerve damage and increases macrophage immunoreactivity. TNT is subsequently used to deliver vasculogenic cell therapies to crushed nerves via delivery of reprogramming factor genes *Etv2*, *Foxc2*, and *Fli1* (*EFF*). The results indicate the TNT-based delivery of *EFF* in a sciatic nerve crush model leads to increased vascularity, reduced macrophage infiltration, and improved recovery in electrophysiological parameters compared to crushed nerves that are TNT-treated with sham/empty plasmids. Altogether, the results indicate that TNT can be a powerful platform nanotechnology for localized nonviral gene delivery to nerve tissue, in vivo, and the deployment of reprogramming-based cell therapies for nerve repair/regeneration.

1. Introduction

Peripheral nerve injuries (PNIs) are often multifaceted and present various degrees of severity, potential ischemia, tissue deficits, etc.^[1,2] In many cases, treatment of the nerve injury is delayed for several weeks to handle more immediate concerns of vascular and orthopedic stabilization, and the prevention of infections.^[3,4] Delaying PNI treatment, however, can result in severe long-term consequences.^[4] Therefore, there is a clear need for early intervention strategies that could either lead to a paradigm shift in PNI treatment, or significantly curve progressive degeneration until surgical management can be performed. Today's treatments for PNI, however, have been greatly informed by direct experiences from old military conflicts.^[5,6] Surgical management typically involves the use of cellular autografts, which possess key cues (e.g., cellular, molecular, structural) to support nerve tissue repair.^[7-13] However, complete

J. T. Moore, L. R. Lemmerman, L. Ortega-Pineda, S. Duarte-Sanmiguel, K. Dathathreya, Prof. N. Higueta-Castro, Prof. D. Gallego-Perez
Department of Biomedical Engineering
The Ohio State University
Columbus, OH 43210, USA
E-mail: gallegoperez.1@osu.edu

C. G. Wier
Department of Neuroscience
The Ohio State University
Columbus, OH 43210, USA
D. J. Dodd, W. R. Lawrence
Biomedical Sciences Graduate Program
The Ohio State University
Columbus, OH 43210, USA
S. Duarte-Sanmiguel
Department of Human Sciences
The Ohio State University
Columbus, OH 43210, USA

 The ORCID identification number(s) for the author(s) of this article can be found under <https://doi.org/10.1002/adbi.202000157>.

L. Diaz-Starokozheva, Prof. N. Higueta-Castro, Prof. D. Gallego-Perez
Department of Surgery
The Ohio State University Wexner Medical Center
Columbus, OH 43210, USA

H. N. Harris, Dr. W. D. Arnold, Dr. S. J. Kolb
Department of Neurology
The Ohio State University Wexner Medical Center
Columbus, OH 43210, USA

Prof. C. K. Sen
School of Medicine
Indiana University
Indianapolis, IN 46202, USA

Dr. I. L. Valerio
Plastic and Reconstructive Surgery
Massachusetts General Hospital
Boston, MA 02114, USA

Dr. S. J. Kolb
Department of Biological Chemistry and Pharmacology
The Ohio State University Wexner Medical Center
Columbus, OH 43210, USA

DOI: 10.1002/adbi.202000157

functional recovery is often hindered due to the extended distance requiring regeneration, and the body's inability to drive endogenous repair processes for prolonged periods of time.^[6] Additional concerns include donor site morbidity and donor tissue scarcity.^[14] While acellular nerve allografts (ANAs) could potentially circumvent these issues, ANAs lack important cues for nerve tissue repair (e.g., Schwann and endothelial cells) and as such have poorer outcomes.^[15–17] Alternative strategies focused on the use of scaffolds or other means typically fail to address distal effects from Wallerian degeneration, and/or fall short in being able to sustain growth over large defects.^[6,18,19] Therefore, alternative approaches combining cellular/molecular and surgical innovation are needed to fully address PNI treatment.

Therapies solely based on the administration of neurotrophic/angiogenic factors have had limited impact.^[20–23] While gene therapies have shown promise in preclinical studies,^[24,25] heavy reliance on viral vectors could hamper widespread clinical implementation due to safety concerns stemming from potentially adverse virus–host interactions/immunity, as well as capsid size constraints.^[26–30] Cell therapy has emerged as a promising alternative strategy for the treatment of nerve injury.^[20,22,31–34] Angiogenic cell therapies, in particular, have attracted a great deal of attention due to the synergistic nature of angiogenesis and neurogenesis during nerve tissue repair/development,^[35–38] with newly formed vasculature, for example, acting as a neurotrophic scaffold to support axonal growth.^[38–40] Most cell therapies developed so far, however, rely on progenitor-like cells, which tend to be scarce and difficult to isolate, or pose major risks in terms of uncontrolled differentiation, tumorigenesis, immunogenicity, etc.^[41–43] Recent advances in direct reprogramming could enable the development of autologous cell therapies that are based on more readily available cell sources (e.g., fibroblasts), and mitigate risks associated with progenitor cells.^[44,45] However, similar to gene therapy, current approaches to reprogramming-based cell therapies are fraught with caveats, including the need for viral vectors and extensive *ex vivo* preprocessing (e.g., isolation, expansion, viral transformation, etc.), precluding them as a solution compatible with early intervention strategies. Thus, novel nonviral tools for gene- and reprogramming-based cell therapies are needed to facilitate early intervention in PNI.

Recently we developed a tissue nanotransfection (TNT) technology to deliver nonviral gene- and reprogramming-based cell therapies to skin tissue, *in vivo*, via nanochannels.^[46] Compared to standard bulk electroporation (BEP), nanochannel-based poration minimizes electric field-driven damage to cells, and leads to enhanced cargo delivery.^[45–52] TNT was successfully used to drive reprogramming-based vasculogenic cell therapies in the skin via codelivery of *Etv2*, *Foxc2*, and *Fli1* (*EFF*) genes, which can induce direct conversion of fibroblasts into induced endothelial cells (iECs).^[46] Here we explored, for the first time, the use of TNT as a platform nanotechnology for the delivery of gene and reprogramming-based cell therapies to peripheral nerve tissue.

2. Results

To examine whether TNT can effectively deliver genetic cargo to peripheral nerves, we proceeded to conduct gene delivery

experiments in the sciatic nerve of 8–10-week-old C57BL/6 mice using fluorescently labeled plasmid DNA (PCMV6, 4.9 kb, Origene) as model cargo (Figure 1). The sciatic nerves were surgically accessed through a longitudinal incision, posterior and parallel to the femur, and the TNT platform was placed against the exposed nerve surface prior to applying a pulsed electric field across electrodes (Figure 1a). TNT conditions included 10 pulses of 200 Volts (V) and a duration of 10 millisecond (ms) per pulse with a 100 ms interval, for a total duration of 1 s per run. The sciatic nerve was collected within 5 min after gene delivery, and subsequently sectioned and processed for inspection via fluorescence microscopy. Imaging of TNT-treated nerve tissue revealed that under these conditions, the delivered plasmid DNA accumulated preferentially within the epineurium (Figure 1d), the outermost layer of the nerve, which is made from dense irregular connective tissue (e.g., collagen, fibroblasts), and plays a key protective role (e.g., mechanical and diffusion barrier) to the underlying axons.^[53–55]

To evaluate if TNT had a negative impact on functionality due to activation of an innate immune response or axonal damage, motor function was assessed 3 days post-TNT via compound muscle action potential (CMAP) measurements recorded from the sciatic innervated triceps surae muscle following sciatic nerve stimulation.^[56,57] Our results indicate that TNT had no detrimental impact on functionality (Figure 1e). To evaluate if standard BEP elicited similar responses, the plasmid solution was first injected into the sciatic nerve, and the nerve trunk was subsequently gently secured between two plate electrodes before applying a bias of 200 V (i.e., 10 pulses of 10 ms each) across electrodes (Figure S1, Supporting Information). Day-3 CMAP measurements for BEP-treated nerve, however, revealed that when the same conditions were applied under a BEP setup, there was a significant (i.e., ~97%) reduction in CMAP amplitude (Figure 1e), clearly suggesting that BEP had a negative impact on neuromuscular function. Simulation studies indicate that nanochannel-based implementation of an electric field results in highly localized tissue poration (Figure 1b,c) compared to BEP (Figure S1, Supporting Information), which presumably has a cytoprotective effect on highly sensitive electrically excitable/electrogenic tissue, such as nerve tissue.^[52] CMAP measurements in mice that had undergone sham surgeries (i.e., exposing the nerve but no TNT or BEP-driven electrical stimulation) revealed that the surgical procedure itself had no detrimental impact on neuromuscular function (Figure S2, Supporting Information), thus suggesting that the decrease in CMAP amplitude was primarily caused by the BEP procedure.

While the cells that reside in the epineurium (e.g., fibroblasts, immune cells) could represent a target of therapeutic interest for a number of conditions (e.g., demyelinating polyneuropathy, vasa nervorum disruption),^[58,59] nonviral delivery of genetic cargo deeper into the nerve could potentially enable a wider range of therapeutic applications, as more cellular/molecular targets become available, including Schwann cells, endothelial cells, fibroblasts, immune cells, etc.^[60,61] Therefore, we proceeded to develop a benign method to gently exfoliate the nerve to remove the epineurial barrier prior to TNT. We found that applying 0.25% trypsin for 5 min to the surgically exposed nerve surface in 8–10-week-old C57BL/6 mice successfully

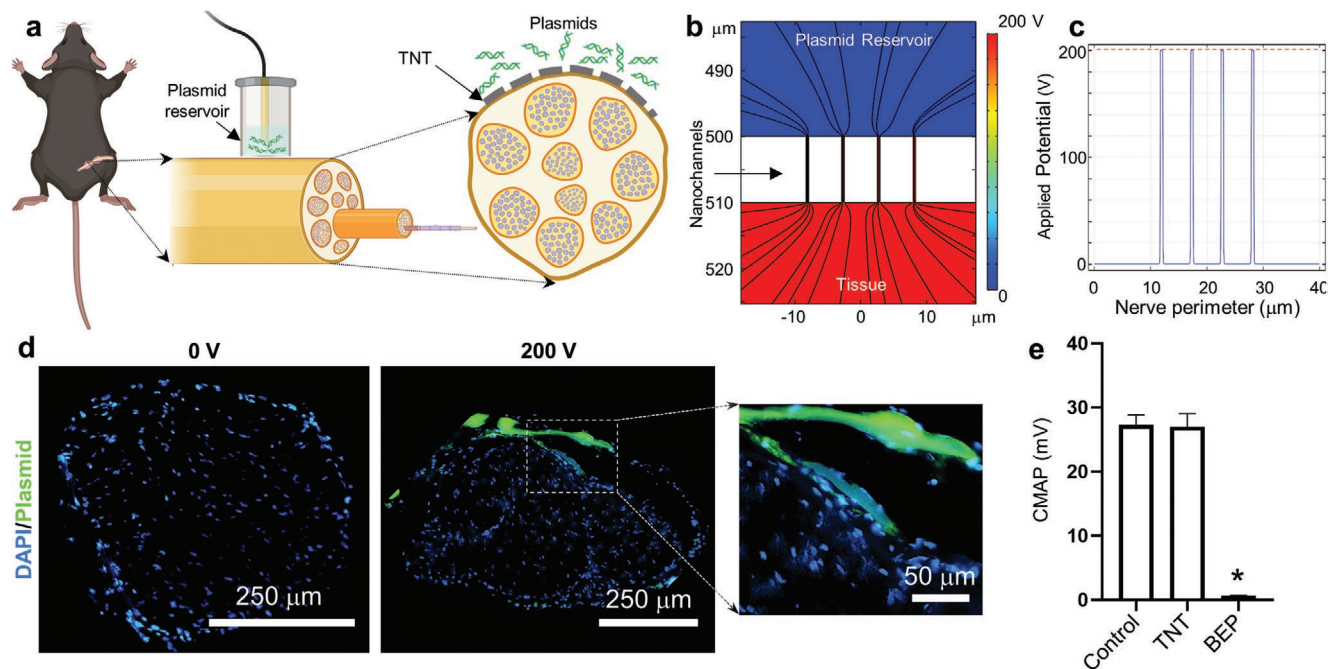


Figure 1. TNT can be used to deliver nucleic acids to genes in a safe and efficient manner. a) Schematic diagram of the experimental procedure. The sciatic nerve is first surgically exposed, and the nanochanneled surface of the TNT platform is put in direct contact with the nerve. A negative electrode is immersed into the plasmid reservoir and a positive electrode is inserted into the muscle adjacent to the nerve. A pulsed electric field is then applied across electrodes to nanoporate the tissue surface and electrophoretically drive nucleic acids into the nerve. b,c) Finite element modeling simulations of the electric field distribution when the poration is mediated by nanochannels. Dashed red line shows the voltage distribution for bulk electroporation. Nanochannel-mediated poration enables focused implementation of the electric field (solid blue line). d) Fluorescence micrograph of the nerve cross-section following TNT with labeled plasmid DNA (green) at 0 versus 200 V. The plasmid DNA accumulates preferentially within the epineurium of the TNT-treated nerve surface. Inset to the right shows higher magnification image of the labeled plasmid within the epineurium. e) Neuromuscular activity was evaluated via compound muscle action potential (CMAP) measurements in mice that underwent surgery to expose the sciatic nerve (control) versus mice that underwent the surgery in addition to TNT- or BEP-based poration of the nerve ($n = 3$). While BEP led to a significant decrease in CMAP amplitude, TNT did not cause any significant changes. Mean \pm sem, $*p < 0.001$ versus control (One Way Anova).

removed the outermost tissue layer of the sciatic nerve (Figure S3, Supporting Information). Functionality tests revealed that the exfoliation treatment had no negative impact on CMAP amplitude (Figure S4, Supporting Information). Moreover, histological analyses performed at days 3 and 7 postexfoliation revealed that the epineurial barrier has the ability to regenerate (Figure S3, Supporting Information). Once we established that the trypsin treatment can be used to benignly and reversibly remove the epineurial barrier, we proceeded to run TNT experiments on exfoliated nerve tissue under different voltage conditions, and using fluorescently labeled plasmid DNA (PCMV6, 4.9 kb, Origene) as model cargo (Figure 2a). The tissue was collected immediately after TNT and processed and analyzed via fluorescence microscopy. Imaging of the nerve tissue sections revealed that the delivery extent of plasmid DNA into the nerve can be modulated by the magnitude of the applied voltage and pulse length (Figure 2b–e). Thus, these results confirm that trypsin-based exfoliation is a viable method to gain access to inner nerve tissue for TNT-driven gene delivery applications.

To further contrast the performance of TNT versus BEP, and to better understand the underlying principles driving impaired functionality in BEP, we proceeded to conduct gene delivery experiments with TNT and BEP at 200 V (i.e., 10 pulses, 10 ms per pulse) in exfoliated sciatic nerves of 8–10-week-old C57BL/6 mice, using plasmid DNA (PCMV6, 4.9 kb, Origene) as model

cargo. Functional outcomes postgene delivery were measured in terms of toe-spread and pinprick response, and histological analyses of nerve damage and inflammatory markers were also conducted at day 3 postgene delivery (Figure 3a). While toe-spread and pinprick assessments indicated that TNT and direct injection of the plasmid into the nerve prior to BEP yielded similar responses compared to untreated healthy control nerve tissue, histological analysis of nerve damage with Fluoro-jade-C (FJ-C) showed that plasmid injection, which is inherently needed for BEP-based gene delivery, can induce some degree of nerve damage (Figure 3b). No FJ-C signal was detected for TNT-treated nerves. In addition, when plasmid injection was followed by BEP at 200 V, histological damage was not only clearly visible by FJ-C staining, but abnormal toe-spread and pinprick response were also recorded in all the mice subjected to BEP (Figure 3a,b). Interestingly, analysis of the macrophage marker, F4/80, and the cellularity of the cross-section, revealed that only the nerves that underwent plasmid injection + BEP showed significantly increased immunoreactivity for F4/80, and a marked decrease in cellularity (i.e., DAPI signal) per cross-section (Figure 3c,d), suggesting that the BEP procedure itself is cytotoxic to the nerve, and is conducive to more prolonged inflammation compared to the TNT procedure or plasmid injection alone, which could potentially contribute to the functional decline seen in the BEP group.^[62–64]

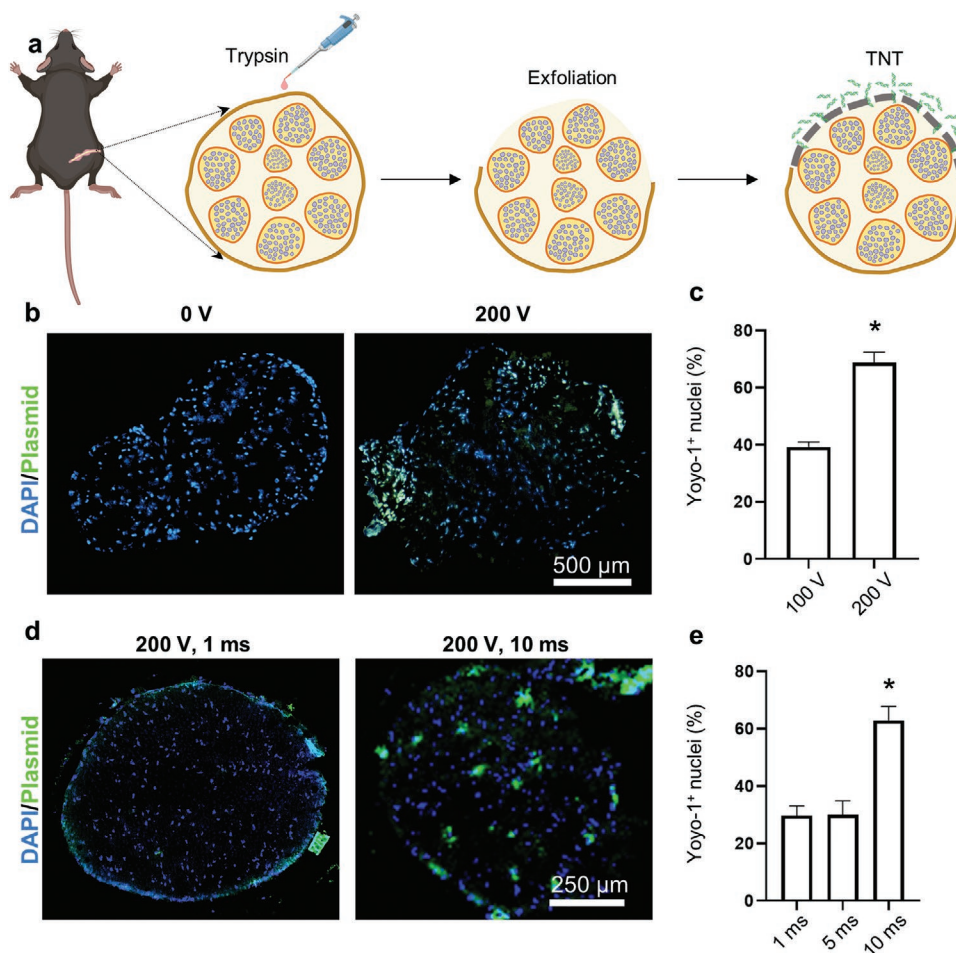


Figure 2. Trypsin treatment gently removes the epineurial membrane and enables nanochannel-mediated delivery of nucleic acids into the nerve core. a) Schematic diagram of the experimental procedure. The exposed sciatic nerve surface is treated with 0.25% trypsin for 5 min to remove the epineurium prior to conducting TNT. The delivery efficiency (% of Yoyo-1⁺ nuclei) can be modulated via the b,c) applied voltage or d,e) pulse length ($n = 3$). Mean \pm sem, * $p < 0.002$.

Once we established that TNT represented a safe and effective approach to deliver genetic cargo into nerve tissue, we proceeded to evaluate whether TNT can be used to drive reprogramming-based vasculogenic cell therapies in injured nerves (Figure 4a). Vasculogenic cell therapies have been shown to improve nerve tissue repair under neurodegenerative conditions.^[35–40] To test this, we first performed a crush injury to the sciatic nerve of 8–10-week-old C57BL/6 mice using well-established procedures.^[65–67] Briefly, the surgically exposed nerve was crushed with locked forceps, applying 2 midlevel crushes for 15 s, with a 15 s release time. This was immediately followed by trypsin-based exfoliation and TNT-based delivery of a vasculogenic reprogramming gene cocktail of *Etv2*, *Foxc2*, and *Fli1* (*EFF*), which we had previously reported to drive vasculogenic cell therapies in the skin.^[46] TNT with sham/empty plasmids served as control. TNT conditions included 10 pulses of 200 V and a duration of 10 ms per pulse. Positive immunoreactivity for the Myc-DDK tag protein coupled with qRT-PCR analyses confirms successful expression of the delivered plasmids (Figure S5, Supporting Information). Histological analyses of the nerve at day 7 postcrush and TNT

indicated that TNT-based delivery of *EFF* correlated with a significant increase in immunoreactivity for vascular markers, vWF and CD31, compared to crushed nerve tissue that was TNT-treated with sham/empty plasmids (Figure 4b,c). No significant differences were noted between crushed/*EFF*-treated nerve and healthy/uncrushed controls (Figure 4c). Notably, when neuromuscular function was evaluated via CMAP measurements, we found that while the crush injury had a clear negative impact on CMAP amplitude at $t = 7$ days postcrush injury, the mice that were treated with *EFF* TNT showed improved and more pronounced recovery as early as $t = 14$ days postinjury compared to baseline measurements at day 7 (Figure 4d). Mice treated with sham TNT, on the other hand, showed significantly reduced recovery in CMAP, suggesting that the TNT-driven vasculogenic intervention had a positive impact on the recovery rate. Analysis of macrophage marker, F4/80, showed that crushed nerve tissue TNT-treated with sham/empty plasmids exhibited more pronounced immunoreactivity compared to crushed nerve tissue TNT-treated with *EFF* and/or healthy/uncrushed nerve (Figure 5a,b). Both sham- and *EFF*-treated nerves showed similarly elevated levels

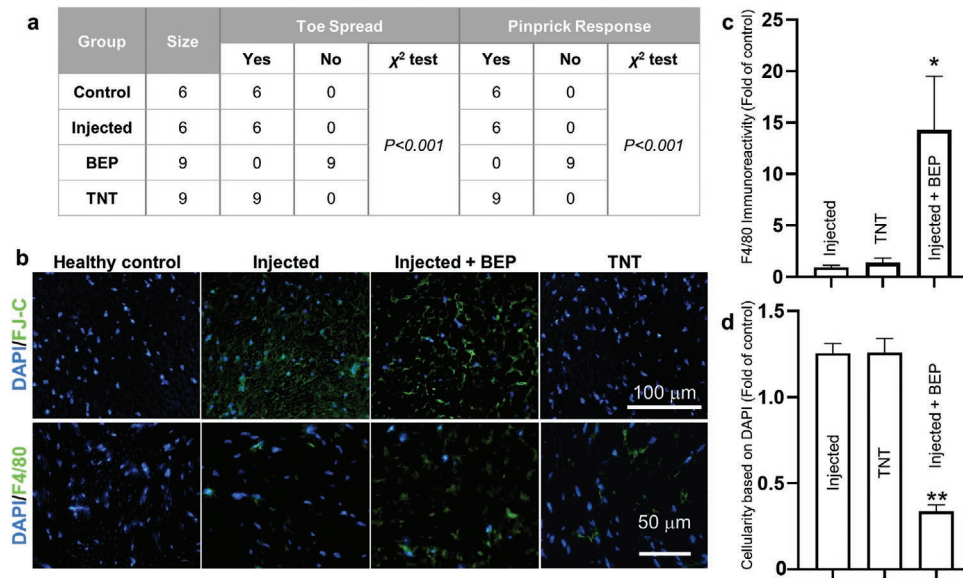


Figure 3. BEP leads to functional impairment, increased macrophage infiltration, and reduced cellularity. a) Assessment of toe-spread and pinprick response in mice subjected to TNT, plasmid injection, and plasmid followed by BEP ($n = 6-9$). Untreated mice served as control. b) Fluorescence micrographs showing histological changes in response to TNT, plasmid injection, and plasmid injection + BEP. While plasmid injection with or without BEP appeared to lead to some degree of histological damage ($t = 3$ days postinjection/BEP), only the BEP group led to a significant increase in c) macrophage marker immunoreactivity (F4/80) ($n = 3-4$), and a d) marked decrease in cellularity ($n = 3$). Mean \pm sem, * $p < 0.05$ ** $p < 0.001$ versus control/healthy nerve tissue (One Way Anova).

of immunoreactivity for S100B at day 7 postinjury/intervention compared to healthy/uncrushed nerves (Figure 5a,c), presumably reflective of increased Schwann cell and fibroblast activity in response to the crush injury.^[68] Immunostaining for axonal marker, neurofilament heavy chain (NF), showed

a significant decrease in immunoreactivity for crushed nerves treated with sham TNT compared to healthy control/uncrushed nerve tissue (Figure 5a,d). No significant differences in NF immunoreactivity were noticed between healthy controls and crushed nerves treated with *EFF* TNT, suggesting

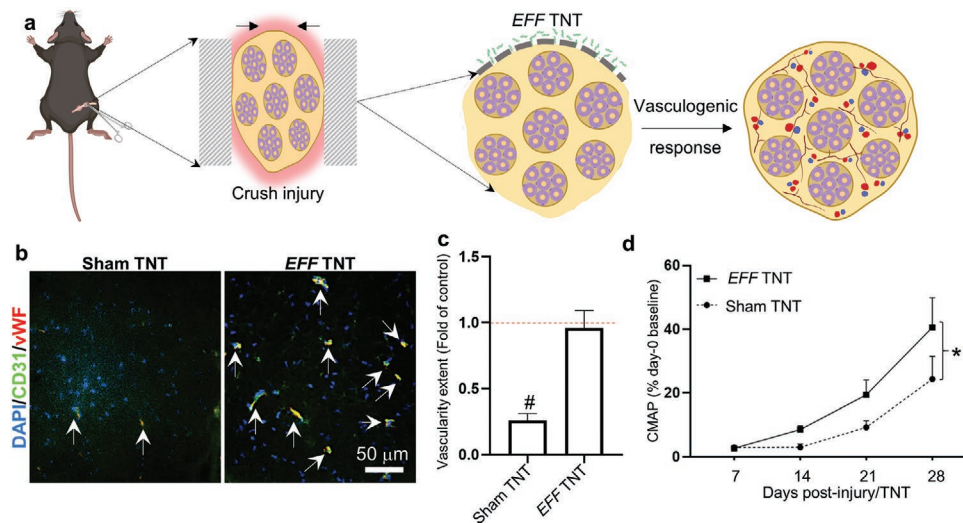


Figure 4. TNT-based delivery of *EFF* to crushed nerve tissue leads to an increase in vascularity and correlates with improved functional outcomes. a) Schematic diagram of the experimental design. The sciatic nerve was crushed, exfoliated, and TNT-treated with *EFF* or sham/control plasmids. Histological changes were evaluated at day 7 postinjury/treatment, and changes in neuromuscular function were assessed via CMAP measurements at days 7–28 postinjury/treatment. b) Histological analysis of vascularity confirmed c) increased immunoreactivity for CD31 and vWF in *EFF*-treated nerves compared to sham ($n = 3$). d) CMAP measurements show significant recovery for both groups over time ($p = 0.0003$) and reveals that TNT-based delivery of *EFF* led to significantly improved recovery compared to baseline measurements ($n = 5-6$). Significant spontaneous recovery in sham-treated mice was not seen until 28 days postinjury. Mean \pm sem, # $p < 0.005$ versus control/healthy nerve tissue (One Way Anova), * $p < 0.05$ (repeat measure, mixed effect analysis).

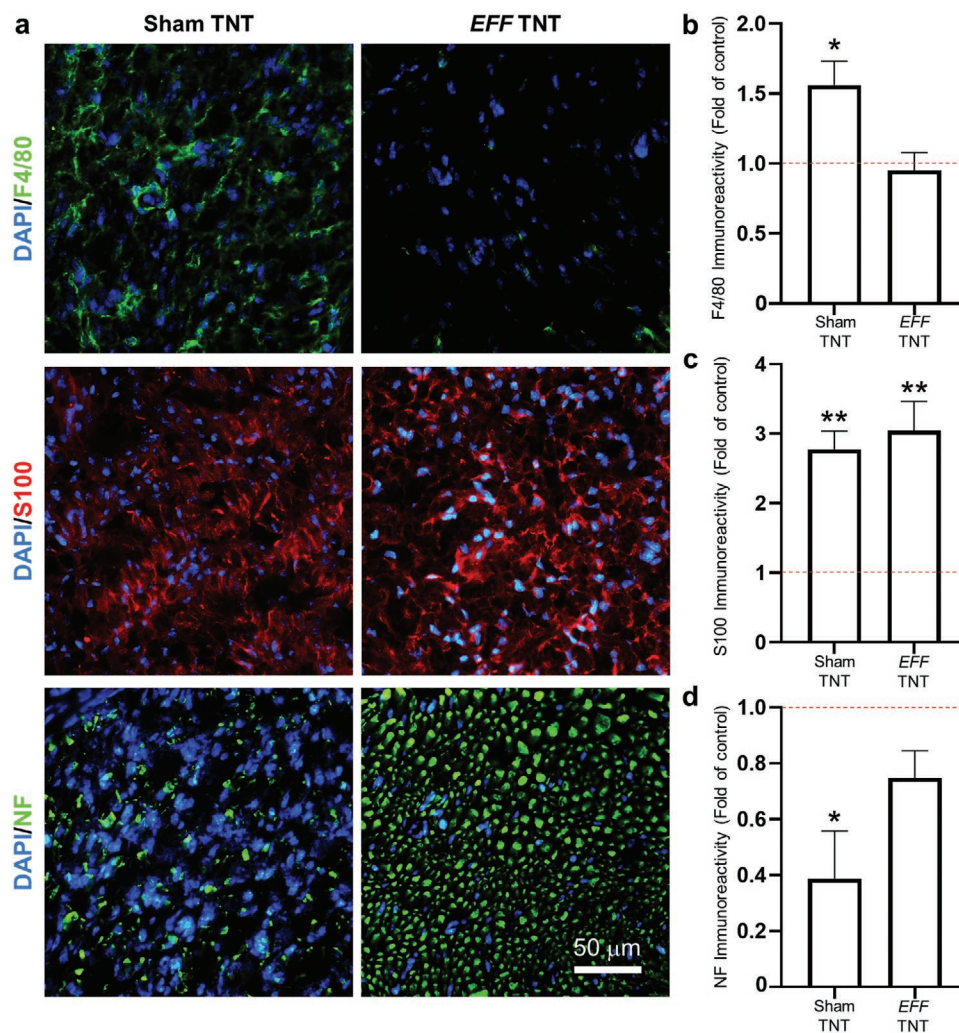


Figure 5. TNT-based delivery of *EFF* to crushed nerve tissue correlates with reduced macrophage infiltration and improved protection/regeneration of axonal processes. a) Immunofluorescence staining and b–d) quantification of F4/80, S100, and Neurofilament (NF) immunoreactivity in sham- versus *EFF*-treated crushed nerve tissue ($n = 3$). Mean \pm sem, $*p < 0.05$ $**p < 0.006$ versus control/healthy nerve tissue (One Way Anova).

that the vasculogenic intervention had a positive impact in the preservation of axonal processes following crush injury.

The increase in vascular tissue immunoreactivity in response to TNT-based delivery of *EFF* is likely due to the combined effect of paracrine angiogenesis from pre-existing blood vessels, and lineage conversions between somatic cells toward an induced endothelial cell (iEC) phenotype.^[46] To investigate the extent to which specific subpopulations of nerve-resident cells were responsive to *EFF*-driven vasculogenic reprogramming, we proceeded to run ex vivo nanoelectroporation (NEP) experiments with *EFF* plasmids and select cell populations of the sciatic nerve.^[45,46] High magnification coimmunofluorescence imaging of vascular markers (e.g., CD31, vWF) and S100B or F4/80 indicate that some of the vascular cells observed in the cross-sections of crushed nerves TNT-treated with *EFF* showed potential traces of S100B immunoreactivity (Figure S6, Supporting Information). No such traces were observed for F4/80, thus suggesting that some of the iECs may be originating from S100B⁺ cell populations. As such, we proceeded to evaluate the reprogrammability of Schwann cell cultures and sciatic nerve

fibroblast cultures into iECs in response to NEP of *EFF*. NEP of sham/empty plasmids served as control. Immunofluorescence analysis of the Schwann cell and fibroblast cultures 7 days post-NEP revealed the presence of cells that stained positive for vascular markers in the fibroblast cultures that were NEP-treated with *EFF* (Figure S6, Supporting Information). No such cells were seen in fibroblast cultures that were NEP-treated with sham/empty plasmids, or Schwann cell cultures NEP-treated with *EFF* or sham plasmids (Figure S6, Supporting Information), thus suggesting that sciatic nerve fibroblasts are more prone to exhibiting vasculogenic plasticity compared to Schwann cells, which could be of relevance to reprogramming-based vasculogenic cell therapies for peripheral nerve tissue.

3. Conclusion

In conclusion, we demonstrated that TNT can be used to safely and effectively deliver genetic cargo to peripheral nerve tissue, nonvirally, which could potentially be used to drive a myriad

Table 1. Plasmid information.

Name	Catalog number	Antibiotic resistance	Vector	Size [kb]	Vendor
PCMV6 (Sham)	PS100010/ PS100001	Ampicillin/ Kanamycin	PCMV6	4.9–6.6	Origene
<i>Etv2</i>	MG216258/ MR216258			5.9–7.6	
<i>Fli1</i>	MG225907/ MR225907			6.2–7.9	
<i>Foxc2</i>	MG221977/ MR221977			6.4–8.0	

of gene and/or cell therapies of relevance to neuropathic and neurodegenerative conditions. Benchmarking studies with BEP indicated that TNT-based delivery of genetic cargo led to little to no damage to the nerve cytoarchitecture, and had negligible impact on inflammatory cell infiltration and neuromuscular function. BEP, on the other hand, caused visible damage to nerve tissue, promoted marked inflammatory cell infiltration, and had a detrimental impact on neuromuscular function, thus suggesting that nanoscale confinement of electroporation in TNT is better suited for electric field-based delivery of genetic cargo to nerve tissue. Subsequent studies in a mouse model of crush nerve injury indicate that TNT-based delivery of a vasculogenic gene cocktail of *Etv2*, *Foxc2*, and *Fli1* (*EFF*), which we had previously reported to mediate reprogramming of dermal fibroblasts into induced endothelial cells,^[46] leads to improved injury outcomes compared to TNT-based intervention with sham/empty plasmids, including increased vascularization, reduced inflammation, improved preservation of axonal processes, and speedier recovery of neuromuscular function. Altogether, these studies suggest that TNT is a powerful platform nanotechnology for nonviral gene delivery to nerve tissue, and the deployment of reprogramming-based cell therapies of potential relevance to a wide variety of conditions.

4. Experimental Section

Plasmid Preparation: All plasmids were purchased from Origene (Table 1). All plasmids were expanded via bacterial inoculation and purified as directed by the protocol for plasmid purification (ZymoPURE II Plasmid Midprep Kit, cat. no. D4201). Concentrations of isolated plasmids were obtained using a Nanodrop 2000c Spectrophotometer (ThermoFisher Scientific). The plasmids were labeled for some experiments using Yoyo-1 Iodide (cat. no. Y3601, ThermoFisher Scientific) following the instructions provided by the manufacturer.

Animal Husbandry: All animal procedures were approved by the Animal Care and Use Committee of The Ohio State University (2016A00000074-R1). C57BL/6 mice were purchased from Jackson Laboratory. Mice were 8–10 weeks at the time of experimentation. Both male and female sexed mice were included in the studies. All animals were anesthetized via isoflurane inhalation before experimental manipulations.

Sciatic Nerve Exposure, Crush Injury, and Gene Delivery: A skin and muscle incision of ≈ 1 cm was made in the medial aspect of the limb to expose the sciatic nerve. Sciatic nerves were separated from the surrounding tissue and fascia using Vannas spring scissors. For the crush injury model, the sciatic nerve was crushed using 1 mm wide hemostatic forceps (3 clicks) 2 times for 15 s. Prior to the second crush, the forceps were dipped in carbon powder to mark the site of injury. For TNT experiments, a track-etched Polyethylene terephthalate (PET) membrane with a pore size of ≈ 400 nm and a density of $\approx 10^8$ pores cm^{-2} was adapted into a TNT platform. The basal surface of the membrane was gently pressed against the sciatic nerve, with the apical compartment/membrane containing the plasmid solution (at

a $0.05 \mu\text{g } \mu\text{L}^{-1}$ per plasmid concentration) and the negative electrode. A positive needle electrode was then inserted into the biceps femoris, and a pulsed electric field (0–200 V, 10 ms pulses, 10 pulses) was applied across electrodes to drive plasmid DNA across the nanochannels and into the nerve. For BEP experiments, the plasmid solution ($0.05 \mu\text{g } \mu\text{L}^{-1}$) was preinjected into the nerve using a 1cc U-100 insulin syringe (BD 329 424). The nerve was subsequently gently clamped between two plate electrodes, and a pulsed electric field (200 V, 10 ms pulses, 10 pulses) was applied across electrodes to facilitate electroporation-based plasmid uptake. Exfoliation (i.e., epineurium removal) of the sciatic nerve was conducted for some experiments by applying 0.25% trypsin (50–100 μL) to the exposed nerve surface for a total of 5 min. The trypsin was then removed via cotton tip applicator prior to DNA delivery experiments. COMSOL Multiphysics version 5.4 was used to study and compare the electric field distribution for both BEP and TNT. Static electric field physics was used to analyze the physical model set up. For BEP, a nerve cross-section of 500 μm was sandwiched between two copper plates and voltage of 200 V was applied. A conductivity of 0.2 S m^{-1} was used for the nerve tissue. For TNT 400 nm diameter and 10 mm long nanochannels in direct contact with the nerve surface were used. Positive electrode was modeled underneath the nerve to replicate the experimental set up. An electric potential of 200 V was applied between the top surface and the positive electrode under the nerve. The conductivity for plasmid, nerve, and membrane were 0.8, 0.2 and $5 \times 10^{-7} \text{ S m}^{-1}$, respectively.^[52]

Nerve Functionality Measurements: Outcomes of toe-spread and pinprick were documented and recorded after visual observations prior to treatment and at the time of tissue collection.^[69] These measurements were reported in a binary manner. Compound muscle action potentials were recorded from the triceps surae muscle using a Sierra Summit EMG System (Cadwell, Kennewick, WA), as previously described.^[70–72] Briefly, stimulation was applied to the sciatic nerve supramaximally. CMAP amplitudes were recorded using two ring electrodes (Catalog # 9013S0312, Natus Neurology, Middleton, WI); the active electrode was positioned over triceps surae muscles, whereas the reference electrode was positioned on the foot in the mid-metatarsal region. A ground electrode was placed on the animal's tail. Amplitudes were measured peak-to-peak.

Immunohistochemistry: Harvested nerve tissue was embedded in optimal cutting temperature (OCT) solution and frozen for cryosectioning. Immunostaining was performed using specific antibodies and standard procedures. Briefly, OCT-embedded tissues were cryosectioned at 10 μm thickness, fixed in cold methanol, and blocked for nonspecific binding with either 10% normal goat serum or 10% BSA. Tissue samples were incubated with specific antibodies diluted in the blocking solutions overnight at 4 °C (Table 2). The signal was visualized by subsequent incubation with appropriate fluorescence-tagged secondary antibodies Alexa 488-tagged α -chicken, 1:200; (Alexa 488-tagged α -mouse, 1:200; Alexa 488-tagged α -rabbit, 1:200; Alexa 568-tagged α -rabbit, 1:200, Alexa 647-tagged α -rat, 1:200) before being counter-stained with DAPI. Images were captured on an inverted fluorescence microscope (Nikon Ti-2e).

Histological Analysis: Quantitative image analysis was performed using ImageJ (National Institutes of Health). Cellularity was calculated as total number of cells mm^{-2} . Briefly, identical sized regions of interest were obtained for each sample and the total number of DAPI⁺ cells counted. The cell count was normalized to the region of interest size and converted from micrometers to millimeters. Nuclear delivery was calculated as the

Table 2. Antibody information.

Target	Company	Catalog number	Species	Dilution
CD31/PECAM-1	BD Pharmigen	550 274	Rat	1:50
DDK (FLAG)	Origene	TA50011	Mouse	1:500
F4/80	ThermoFisher	14-4801-85	Rat	1:50
Neurofilament heavy polypeptide (NF-H)	Abcam	ab72996	Chicken	1:400
S100B	Abcam	ab52642	Rabbit	1:500
Von Willebrand Factor (vWF)	Abcam	ab6994	Rabbit	1:500

ratio of localized Yoyo-1⁺ and DAPI⁺ nuclei to the total number of DAPI⁺ cells/nuclei. Briefly, ImageJ was used to manually count DAPI⁺ cells/nuclei and DAPI⁺/Yoyo-1⁺ nuclei. The total for each population was recorded and a ratio/percentage for Yoyo-1⁺ nuclei was presented. Immunoreactivity analysis was calculated as the area of immunostained nerve tissue. Briefly, images were split by channel and converted to binary images. A threshold algorithm was applied and the sum of positive particles calculated as a percent coverage of the nerve bundle. To calculate vascular coverage, the CD31⁺ and vWF⁺ regions were manually traced. The areas of the costained regions were summed and converted to a ratio of coverage of the nerve bundle. All analyses were compared to healthy controls and represented as a ratio/fold-change of the normal state. Each analysis was performed based on the average results of 3–4 tissue sections/images from 3 to 4 biological replicates per group.

In Vitro Reprogramming Assays: To evaluate whether specific cell populations from the nerve were susceptible to reprogramming, in vitro reprogramming experiments Schwann cells (CRL-2766, ATCC) and primary sciatic nerve fibroblasts were conducted.^[73] The *EFF* (*Etv2*, *Foxc2*, *Fli1*) or sham/empty PCMV6 plasmids were delivered into the cells via nanochannel-based or standard electroporation approaches, as described elsewhere.^[45,46] The cells were maintained in culture for an additional 7 days postgene delivery, and then processed for immunostaining against vascular markers, as described above with few modifications. Briefly, the cells were fixed in a 10% formalin solution and permeabilized via 0.1% Triton X-100. Cells were then washed and immunostained.

Gene Expression: Sections of sciatic nerves were used to evaluate transcription factor expression after TNT. Samples were placed in TRIzol reagent (ThermoFisher Scientific, ref. no. 15 596 026) and total RNA was extracted according to the manufacturer's protocol. Subsequently, cDNA was generated through a reverse-transcriptase reaction using SuperScript IV VILO Master Mix (ThermoFisher Scientific, ref. no. 11 756 500). Targets were detected using FAM labeled TaqMan probes (Table 3; ThermoFisher Scientific) and the QuantStudio 3 Real-Time PCR System (ThermoFisher Scientific). Relative transcript levels were reported as $\Delta\Delta CT$ values, where $\Delta\Delta CT$ is $\Delta CT_{Treated} - \Delta CT_{Control/Untreated}$.

Statistical Analysis: When possible, coding was used for samples, and blinding introduced in data collection. Reported data were represented as the mean \pm standard error of 3–9 biological replicates. In the case of unsuccessful gene delivery or misfires (potentially the result of

poor connection between the nanochannels and nerve, or clogging of nanochannels), results were excluded from the analysis. Experiments were replicated at least twice to confirm reproducibility. Comparisons between groups were made by analysis of variance (ANOVA). Statistical differences were determined using parametric/nonparametric tests, as appropriate, with SigmaPlot version 14.0. Toe-spread and pinprick data were then evaluated using a chi-square analysis.

Supporting Information

Supporting Information is available from the Wiley Online Library or from the author.

Acknowledgements

Funding for this work was provided by NIH/NIBIB via a New Innovator Award to D.G.-P. (DP2EB028110) and NIH/NINDS (R21NS099869).

Conflict of Interest

The authors declare no conflict of interest.

Author Contributions

The idea was conceived by D.G.-P., N.H.-C., and S.J.K. Gene delivery experiments and histological analyses were conducted by J.T.M., C.G.W., L.R.L., L.O.-P., D.J.D., W.R.L., S.D.-S., and L.D.-S. Simulations were run by K.D., J.T.M., and D.G.-P. Neuromuscular function assessments were conducted by J.T.M., C.G.W., H.N.H., S.J.K., and W.D.A. Crush injury model and TNT-based intervention strategy was designed and implemented by J.T.M., D.G.-P., and N.H.-C., with support/guidance from C.K.S., I.L.V., S.J.K., and W.D.A. The manuscript was written by D.G.-P. and J.T.M. with the support from N.H.-C., S.J.K., and W.D.A.

Table 3. Primer information.

Gene symbol	Gene name	Gene Aliases	Species	Company	Ref. no.
<i>GAPDH</i>	glyceraldehyde-3-phosphate dehydrogenase	Gapd	Mouse	ThermoFisher Scientific	Mm99999915_g1
<i>Etv2</i>	ets variant 2	Etsrp71	Mouse	ThermoFisher Scientific	Mm00468389_m1
<i>Fli1</i>	Friend leukemia integration 1	EWSR2, Fli-1, SIC-1, Sic1	Mouse	ThermoFisher Scientific	Mm00484410_m1
<i>Foxc2</i>	forkhead box C2	Fkh14, Hfhb3, MFH-1, Mfh1	Mouse	ThermoFisher Scientific	Mm00546194_s1

Keywords

nonviral gene delivery, peripheral nerve, tissue nanotransfection

Received: June 18, 2020

Revised: August 4, 2020

Published online: September 16, 2020

- [1] H. I. Secer, I. Solmaz, I. Anik, Y. Izci, B. Duz, M. K. Daneyemez, E. Gonul, *J. Brachial Plex. Peripher. Nerve Inj.* **2009**, 4, 11.
- [2] K. Burt, I. Badash, B. Wu, *Clin. Trials Orthop. Disord.* **2017**, 2, 123.
- [3] J. M. Ecklund, G. S. Ling, *Neurosurg. Clin. North Am.* **2009**, 20, 107.
- [4] J. K. Smith, M. E. Miller, C. G. Carroll, W. J. Faillace, L. J. Nesti, C. M. Cawley, M. E. Landau, *Muscle Nerve* **2016**, 54, 1139.
- [5] N. J. Naff, J. M. Ecklund, *Neurosurg. Clin.* **2001**, 12, 197.
- [6] A. D. Gaudet, P. G. Popovich, M. S. Ramer, *J. Neuroinflammation* **2011**, 8, 110.
- [7] R. V. Weber, S. E. Mackinnon, *Clin. Plast. Surg.* **2005**, 32, 605.
- [8] R. P. Bunge, *Curr. Opin. Neurobiol.* **1993**, 3, 805.
- [9] A. D. Levi, V. Guenard, P. Aebischer, R. P. Bunge, *J. Neurosci.* **1994**, 14, 1309.
- [10] A. D. Levi, V. K. Sonntag, C. Dickman, J. Mather, R. H. Li, S. C. Cordoba, B. Bichard, M. Berens, *Exp. Neurol.* **1997**, 143, 25.
- [11] J. L. Bixby, J. Lilien, L. F. Reichardt, *J. Cell Biol.* **1988**, 107, 353.
- [12] E. L. Whitlock, S. H. Tuffaha, J. P. Luciano, Y. Yan, D. A. Hunter, C. K. Magill, A. M. Moore, A. Y. Tong, S. E. Mackinnon, G. H. Borschel, *Muscle Nerve* **2009**, 39, 787.
- [13] N. J. Jesuraj, K. B. Santosa, M. R. Macewan, A. M. Moore, R. Kasukurthi, W. Z. Ray, E. R. Flagg, D. A. Hunter, G. H. Borschel, P. J. Johnson, S. E. Mackinnon, S. E. Sakiyama-Elbert, *Muscle Nerve* **2014**, 49, 267.
- [14] X. Sun, Y. Wang, Z. Guo, B. Xiao, Z. Sun, H. Yin, H. Meng, X. Sui, Q. Zhao, Q. Guo, A. Wang, W. Xu, S. Liu, Y. Li, S. Lu, J. Peng, *Adv. Healthcare Mater.* **2018**, 7, 1800276.
- [15] M. Saheb-Al-Zamani, Y. Yan, S. J. Farber, D. A. Hunter, P. Newton, M. D. Wood, S. A. Stewart, P. J. Johnson, S. E. Mackinnon, *Exp. Neurol.* **2013**, 247, 165.
- [16] T. J. Best, S. E. Mackinnon, P. J. Evans, D. Hunter, R. Midha, *J. Reconstr. Microsurg.* **1999**, 15, 183.
- [17] J. M. Rovak, A. K. Mungara, M. A. Aydin, P. S. Cederna, *J. Reconstr. Microsurg.* **2004**, 21, 53.
- [18] A. Faroni, S. A. Mobasseri, P. J. Kingham, A. J. Reid, *Adv. Drug Delivery Rev.* **2015**, 82–83, 160.
- [19] A. Muheremu, Q. Ao, *Biomed. Res. Int.* **2015**, 2015, 237507.
- [20] J. O. Jeong, M. O. Kim, H. Kim, M. Y. Lee, S. W. Kim, M. Ii, J. U. Lee, J. Lee, Y. J. Choi, H. J. Cho, N. Lee, M. Silver, A. Wecker, D. W. Kim, Y. S. Yoon, *Circulation* **2009**, 119, 699.
- [21] G. Pittenger, A. Vinik, *Exp. Diabetes Res.* **2003**, 4, 271.
- [22] J. W. Han, M. Y. Sin, Y.-s. Yoon, *Diabetes Metab. J.* **2013**, 37, 91.
- [23] G. Terenghi, *J. Anatomy* **1999**, 194, 1.
- [24] Y. Wang, W.-Y. Li, P. Sun, Z.-s. Jin, G.-b. Liu, L.-X. Deng, L.-X. Guan, *Neurol. Res.* **2016**, 38, 242.
- [25] S. Zacchigna, M. Giacca, *Int. Rev. Neurobiol.* **2009**, 87, 381.
- [26] S. Daya, K. I. Berns, *Clin. Microbiol. Rev.* **2008**, 21, 583.
- [27] M. Sudres, S. Ciré, V. Vasseur, L. Brault, S. Da Rocha, F. Boisgérault, C. Le Bec, D. A. Gross, V. Blouin, B. Ryffel, *Mol. Ther.* **2012**, 20, 1571.
- [28] M. Ferrand, S. Da Rocha, G. Corre, A. Galy, F. Boisgerault, *Mol. Ther.* **2015**, 23, 1022.
- [29] L. E. Mays, J. M. Wilson, *Mol. Ther.* **2011**, 19, 16.
- [30] B. Greenberg, J. Butler, G. Felker, P. Ponikowski, A. Voors, J. Pogoda, R. Provost, J. Guerrero, R. Hajjar, K. Zsebo, *Gene Ther.* **2016**, 23, 313.
- [31] Y. Li, Z. Zhang, H. S. Kim, S. Han, S. W. Kim, *Mol. Cell. Neurosci.* **2014**, 62, 60.
- [32] S. Walsh, R. Midha, *Neurosurgery* **2009**, 65, A80.
- [33] M. Kitada, T. Murakami, S. Wakao, G. Li, M. Dezawa, *Glia* **2019**, 67, 950.
- [34] Z. Zhao, Y. Wang, J. Peng, Z. Ren, S. Zhan, Y. Liu, B. Zhao, Q. Zhao, L. Zhang, Q. Guo, *Microsurgery* **2011**, 31, 388.
- [35] K. Arai, E. H. Lo, *J. Neurosci.* **2009**, 29, 4351.
- [36] J. J. Ohab, S. Fleming, A. Blesch, S. T. Carmichael, *J. Neurosci.* **2006**, 26, 13007.
- [37] A. Taguchi, T. Soma, H. Tanaka, T. Kanda, H. Nishimura, H. Yoshikawa, Y. Tsukamoto, H. Iso, Y. Fujimori, D. M. Stern, H. Naritomi, T. Matsuyama, *J. Clin. Invest.* **2004**, 114, 330.
- [38] P. Thored, J. Wood, A. Arvidsson, J. Cammenga, Z. Kokaia, O. Lindvall, *Stroke* **2007**, 38, 3032.
- [39] F. R. Pereira Lopes, B. C. Lisboa, F. Frattini, F. M. Almeida, M. A. Tomaz, P. K. Matsumoto, F. Langone, S. Lora, P. A. Melo, R. Borojevic, S. W. Han, A. M. Martinez, *Neuropathol. Appl. Neurobiol.* **2011**, 37, 600.
- [40] A.-L. Cattin, J. J. Burden, L. Van Emmenis, F. E. Mackenzie, J. J. Hoving, N. G. Calavia, Y. Guo, M. McLaughlin, L. H. Rosenberg, V. Quereda, *Cell* **2015**, 162, 1127.
- [41] H. Okano, M. Nakamura, K. Yoshida, Y. Okada, O. Tsuji, S. Nori, E. Ikeda, S. Yamanaka, K. Miura, *Circ. Res.* **2013**, 112, 523.
- [42] U. Ben-David, N. Benvenisty, *Nat. Rev. Cancer* **2011**, 11, 268.
- [43] A. Bongso, C. Y. Fong, K. Gauthaman, *J. Cell. Biochem.* **2008**, 105, 1352.
- [44] T. Vierbuchen, M. Wernig, *Nat. Biotechnol.* **2011**, 29, 892.
- [45] D. Gallego-Perez, J. J. Otero, C. Czeisler, J. Ma, C. Ortiz, P. Gygli, F. P. Catacutan, H. N. Gokozan, A. Cowgill, T. Sherwood, S. Ghatak, V. Malkoc, X. Zhao, W. C. Liao, S. Gnyawali, X. Wang, A. F. Adler, K. Leong, B. Wulff, T. A. Wilgus, C. Askwith, S. Khanna, C. Rink, C. K. Sen, L. J. Lee, *Nanomedicine* **2016**, 12, 399.
- [46] D. Gallego-Perez, D. Pal, S. Ghatak, V. Malkoc, N. Higueta-Castro, S. Gnyawali, L. Chang, W.-C. Liao, J. Shi, M. Sinha, *Nat. Nanotechnol.* **2017**, 12, 974.
- [47] P. E. Boukany, A. Morss, W. C. Liao, B. Henslee, H. Jung, X. Zhang, B. Yu, X. Wang, Y. Wu, L. Li, K. Gao, X. Hu, X. Zhao, O. Hemminger, W. Lu, G. P. Lafyatis, L. J. Lee, *Nat. Nanotechnol.* **2011**, 6, 747.
- [48] L. Chang, P. Bertani, D. Gallego-Perez, Z. Yang, F. Chen, C. Chiang, V. Malkoc, T. Kuang, K. Gao, L. J. Lee, W. Lu, *Nanoscale* **2015**, 8, 243.
- [49] L. Chang, D. Gallego-Perez, X. Zhao, P. Bertani, Z. Yang, C. L. Chiang, V. Malkoc, J. Shi, C. K. Sen, L. Odonnell, J. Yu, W. Lu, L. J. Lee, *Lab Chip* **2015**, 15, 3147.
- [50] X. Zhao, Y. Wu, D. Gallego-Perez, K. J. Kwak, C. Gupta, X. Ouyang, L. J. Lee, *Anal. Chem.* **2015**, 87, 3208.
- [51] X. Zhao, X. Huang, X. Wang, Y. Wu, A.-K. Eisfeld, S. Schwind, D. Gallego-Perez, P. E. Boukany, G. I. Marcucci, L. J. Lee, *Adv. Sci.* **2015**, 2, 1500111.
- [52] L. Chang, D. Gallego-Perez, C. L. Chiang, P. Bertani, T. Kuang, Y. Sheng, F. Chen, Z. Chen, J. Shi, H. Yang, X. Huang, V. Malkoc, W. Lu, L. J. Lee, *Small* **2016**, 12, 5971.
- [53] Q. Liu, X. Wang, S. Yi, *Front. Neurosci.* **2018**, 12, 597.
- [54] S. Peltonen, M. Alanne, J. Peltonen, *Tissue Barriers* **2013**, 1, e24956.
- [55] K. S. Topp, B. S. Boyd, *Phys. Ther.* **2006**, 86, 92.
- [56] R. M. Menorca, T. S. Fussell, J. C. Elfar, *Hand Clin.* **2013**, 29, 317.
- [57] E. Ydens, A. Cauwels, B. Asselbergh, S. Goethals, L. Peeraer, G. Lornet, L. Almeida-Souza, J. A. Van Ginderachter, V. Timmerman, S. Janssens, *J. Neuroinflammation* **2012**, 9, 176.
- [58] A. K. Mausberg, F. Szepanowski, F. Odoardi, A. Flügel, C. Kleinschmitz, M. Stettner, B. C. Kieseier, *J. Neuroinflammation* **2018**, 15, 217.
- [59] A. Mizisin, A. Weerasuriya, *Acta Neuropathol.* **2011**, 121, 291.
- [60] D. W. Zochodne, *Neurobiology of Peripheral Nerve Regeneration*, Cambridge University Press, Cambridge **2008**.
- [61] W. Jurecka, H. Ammerer, H. Lassmann, *Acta Neuropathol.* **1975**, 32, 299.
- [62] G. Pongratz, R. H. Straub, *Nat. Rev. Rheumatol.* **2013**, 9, 117.

- [63] D. Schomberg, M. Ahmed, G. Miranpuri, J. Olson, D. K. Resnick, *Ann. Neurosci.* **2012**, *19*, 125.
- [64] N. Moreau, A. Mauborgne, S. Bourgoïn, P.-O. Couraud, I. A. Romero, B. B. Weksler, L. Villanueva, M. Pohl, Y. Boucher, *PAIN* **2016**, *157*, 827.
- [65] Y. Gao, C. Weng, X. Wang, *Neural Regener. Res.* **2013**, *8*, 1041.
- [66] J. M. Jacobs, L. S. Ro, *J. Neurol. Sci.* **1994**, *127*, 143.
- [67] M. S. Ju, C. C. Lin, J. L. Fan, R. J. Chen, *J. Biomech.* **2006**, *39*, 97.
- [68] I. Napoli, L. A. Noon, S. Ribeiro, A. P. Kerai, S. Parrinello, L. H. Rosenberg, M. J. Collins, M. C. Harrisingh, I. J. White, A. Woodhoo, *Neuron* **2012**, *73*, 729.
- [69] T. D. Wilder-Kofie, C. Lúquez, M. Adler, J. K. Dykes, J. D. Coleman, S. E. Maslanka, *Comp. Med.* **2011**, *61*, 235.
- [70] J. Li, T. R. Geisbush, W. D. Arnold, G. D. Rosen, P. G. Zaworski, S. B. Rutkove, *PLoS One* **2014**, *9*, e111428.
- [71] W. D. Arnold, K. A. Sheth, C. G. Wier, J. T. Kissel, A. H. Burghes, S. J. Kolb, *J. Visualized Exp.* **2015**, *25*, 52899.
- [72] W. D. Arnold, P. N. Porensky, V. L. McGovern, C. C. Iyer, S. Duque, X. Li, K. Meyer, L. Schmelzer, B. K. Kaspar, S. J. Kolb, J. T. Kissel, A. H. Burghes, *Ann. Clin. Transl. Neurol.* **2014**, *1*, 34.
- [73] Y. Wang, D. Li, G. Wang, L. Chen, J. Chen, Z. Liu, Z. Zhang, H. Shen, Y. Jin, Z. Shen, *Int. J. Biol. Sci.* **2017**, *13*, 1507.